

# Comparative Analysis of Earthquake Detection Methods Using Deep Learning: Reproducibility and Uncertainty Assessment in EQTransformer

Sebastián Gamboa-Chacón<sup>a,x</sup>, Esteban Meneses<sup>a</sup> and Esteban J. Chaves<sup>b</sup>

<sup>a</sup>Costa Rica Institute of Technology and National High Technology Center

<sup>b</sup>Volcanological and Seismological Observatory of Costa Rica, OVSICORI, Universidad Nacional

## ARTICLE INFO

### Keywords:

AI Earthquake detection  
Deep learning  
EQTransformer  
Reproducibility  
Determinism

## ABSTRACT

This study evaluates the performance and reliability of earthquake detection using the EQTransformer, a novel AI program that is widely used in seismological observatories and research for enhancing earthquake catalogs. We test the EQTransformer capabilities and uncertainties using seismic data from the Volcanological and Seismological Observatory of Costa Rica and compare two detection options: the simplified method (MseedPredictor) and the complex method (Predictor), the latter incorporating Monte Carlo Dropout, to assess their reproducibility and uncertainty in identifying seismic events. Our analysis focuses on 24 hour-duration data that began on February 18, 2023, following a magnitude 5.5 mainshock. Notably, we observed that sequential experiments with identical data and parametrization yield different detections and a varying number of events as a function of time. The results demonstrate that the complex method, which leverages iterative dropout, consistently yields more reproducible and reliable detections than the simplified method, which shows greater variability and is more prone to false positives. This study highlights the critical importance of method selection in deep learning models for seismic event detection, emphasizing the need for rigorous evaluation of detection algorithms to ensure accurate and consistent earthquake catalogs and interpretations. Our findings provide valuable insights for the application of AI tools in seismology, particularly in enhancing the precision and reliability of seismic monitoring efforts.

## Credit authorship contribution statement

**Sebastián Gamboa-Chacón:** Conducted the experimental process and programming, as well as the writing of the manuscript. **Esteban Meneses:** Oversaw the project and was responsible for the analysis of the manuscript, including formatting and content corrections from a computational perspective. **Esteban J. Chaves:** Supervised the project and handled the analysis of the manuscript, including formatting and content corrections from a physical and seismological perspective.

## 1. Introduction

Technological advancements in conjunction with theoretical frameworks have revolutionized our understanding of the Earth interior and our ability to interact with it. In seismology, for instance, observatories all over the world, have exponentially increased the number of ultra-sensitive broadband instruments, fiber-optics, nodal arrays and the computational power for archiving and processing data with the aim of improving earthquake detection capabilities,

ORCID(s): 0009-0006-6858-143X (S. Gamboa-Chacón)

<sup>x</sup>Corresponding author. National High Technology Center (CeNAT), 1.3 km north of the United States Embassy, San José, 10109, Costa Rica.

<sup>x</sup>E-mail: sgamboa@cenat.ac.cr.

Code availability: <https://github.com/SebasGamboa10/Reproducibility-and-Uncertainty-Assessment-in-EQTransformer.git>

**This manuscript is a non-peer-reviewed preprint that has been submitted to EarthArXiv. The paper has been submitted to Computers & Geosciences Journal for peer review.**

specifically of smaller magnitude ( $0 \leq M \leq 3.0$ ) events that occur along fault segments and may precede large and catastrophic ruptures [Spassiani and Sebastiani (2016)]. The systematic increase in data since early and middle 2000s, when the digital era began for most seismological networks [Arrowsmith et al. (2022)], have provided researchers with abundant information about the internal structure of the Earth, more complete earthquake catalogs and high quality recordings that allow to better understand fault mechanics and earthquake rupture dynamics.

However, this revolution comes at a cost. The total number of tebibytes of seismological data continues to increase in real time. As a result, traditional methods for earthquake detection and location, which are led by human intervention, are no longer sufficient. These methods struggle to fully capture the number of events generated during an earthquake sequence, especially the smaller magnitude earthquakes. These smaller events are generally obscured by ambient seismic noise, which has comparable frequencies and amplitudes. Machine learning algorithms and artificial intelligence (AI) have significantly enhanced the ability of seismological observatories to detect and estimate earthquake hypocenter locations and magnitudes [Gürsoy et al. (2023)]. All these efforts have been potentiated by high-performance computing (HPC), enabling the scientific institutions to handle resource-intensive tasks, reducing execution times, thereby expediting scientific studies, interpretations and hazard assessments [Hassan et al. (2020)].

Among the innovative algorithms that have been developed, EQTransformer [Mousavi et al. (2020)] (hereafter referred to as EQT), a deep learning-based model, was designed to detect, phase-pick, and associate earthquakes from continuous seismic data. EQT leverages the power of deep learning to analyze seismic signals, offering an efficient and automated solution for earthquake detection. The EQT neural network has a multi-task structure with a deep encoder and three separate decoders. It uses 1D convolutions, bidirectional and unidirectional LSTMs, Network-in-Network, residual connections, self-attentive layers, and transformers. The encoder processes seismic signals and generates high-level representations, while the decoders convert these representations into probability sequences for detecting earthquake signals and the P and S phase arrivals.

One of the novel features of EQT is its ability to provide uncertainties for the detection probabilities, making the results more reliable. These uncertainties are approximated using a Gaussian distribution obtained through Monte Carlo Dropout. Gal and Ghahramani (2016) proposed this method, which reinterprets dropout in deep neural networks as approximate Bayesian inference in deep Gaussian processes, enabling model uncertainty estimation without the computational expense of traditional Bayesian methods. This approach involves applying dropout during both training and inference, performing multiple forward passes to approximate the predictive distribution, and leveraging the variability in these predictions to gauge uncertainty. This method maintains computational efficiency and enhances test accuracy.

For earthquake detection and phase-picking, EQT provides two primary execution methods: a high-level method, referred to in the source code as Predictor (hereafter referred to as Complex), which allows the configuration of multiple

128 parameters for robust execution, and a low-level method, referred to in the source code as MseedPredictor (hereafter  
129 referred to as Simplified), designed for basic execution with fewer adjustable options. Several studies [Jiang et al.  
130 (2021), Pita-Sllim et al. (2023)] have shown promising results when using EQT, enhancing earthquake catalogs and  
131 providing a robust of seismotectonic characterization across different regions. Furthermore, several efforts [van der  
132 Laar et al. (2021), Castillo et al. (2024)] that incorporate EQT methods have been developed aiming to generate auto-  
133 matic pipelines for daily seismological routines.

134 Nevertheless, little to none attention to EQT detection uncertainties and intricacies between the simplified and com-  
135 plex method have been investigated yet. Understanding the differences in performance and behavior between these two  
136 methods is essential for optimizing the use of EQT in various applications but also to generate realistic interpretations  
137 in seismological studies. This work aims to analyze, quantify and describe uncertainties in earthquake detection by  
138 EQTransformer. Reproducibility is a crucial aspect in scientific research, as accurate and consistent results are essential  
139 for researchers studying and analyzing critical characteristics of earthquakes and their uncertainties. Reproducibility  
140 is closely tied to deterministic outcomes, where consistent results are expected for identical experiments, identical data  
141 or algorithm runs. However, our observations clearly show variability in earthquake detection as a function of time  
142 when performing different executions of EQT while maintaining all input variables, data and computer architectures.  
143 We aim to understand the factors contributing to this non-determinism and quantify its impact on the accuracy and  
144 reliability of EQT performance.

145 We analyzed the behavior of EQT focusing on the differences between the simplified and complex execution meth-  
146 ods, particularly, the non-systematic earthquake detection effects introduced by the Monte Carlo Dropout. Given the  
147 complex nature of deep learning models, it is crucial to assess whether their execution is deterministic, that is, whether  
148 identical conditions yield consistent results in repeated runs. To achieve these objectives, we conducted a series of ex-  
149 periments comparing the outputs of EQT using both methods under varying computational setups. By systematically  
150 evaluating the results, we identified variations directly linked to the performance and nature of both algorithms. Not  
151 only does this analysis contribute to a deeper understanding of EQT's functionality and uncertainty, but also provides  
152 insights into the broader implications of using deep learning models for enhancing seismological catalogs.

## 153 2. Background

154 Costa Rica is part of the Central America volcanic front, where four tectonic plates (the Cocos plate, the Caribbean  
155 plate, the Panama microplate, and the Nazca plate) interact along the Middle America Trench [Protti et al. (1994), Mon-  
156 tero et al. (1998)]. The local stress field, induced by this complex geodynamic system into the country, is translated  
157 into hundreds of very active tectonic faults with different length, geometry and seismic potential [Montero et al. (1998),  
158 Styron et al. (2020)]. The Volcanological and Seismological Observatory of Costa Rica (OVSICORI) at Universidad

**Table 1**  
Classification Metrics

Metric	Result
Precision	0.8214
Recall	1.0000
F1-Score	0.9020

159 Nacional operates the largest and most modern geodynamic network in Central America and the Caribbean, composed  
 160 by more than 200 instruments between broadband seismic stations, accelerometers, GNSS and multi-gas, for the per-  
 161 manent monitoring of the tectonic and volcanic activity in the country, generating alerts and official communications  
 162 with governmental institutions and the general public.

163 In 2021, OVSICORI teamed up with the Costa Rica National High Technology Center (CeNAT), developing a  
 164 novel pipeline for identifying and locating earthquakes from waveforms recorded by seismological stations along the  
 165 country van der Laet et al. (2021). Figure 1 summarizes the multiple steps carry out by this pipeline, which relies  
 166 on the capabilities of the EQT algorithm. The classification metrics of the EQT model were assessed to evaluate its  
 167 detection capabilities by analyzing a large aftershock sequence during five days of recording at multiple stations located  
 168 in southern Costa Rica and comparing it with the traditional detection processes developed by OVSICORI. The key  
 169 metrics are Precision, Recall, and F1 Score, summarized also in Table 1 [van der Laet et al. (2021)].

170 Precision, with a value of 0.8214, indicates that 82.14% of the events detected by the EQT model were true positives,  
 171 meaning actual earthquakes. This suggests that there is a 17.86% rate of false positives, where non-seismic events were  
 172 incorrectly identified as earthquakes. Recall is perfect at 1.0000, signifying that the EQT model successfully detected  
 173 all actual earthquake events that occurred during the period of study. The absence of false negatives is crucial for  
 174 comprehensive seismic monitoring, ensuring no real events were missed.

175 The F1 Score, calculated as the harmonic mean of Precision and Recall, stands at 0.9020. This high F1 Score  
 176 reflects a balanced performance of the EQT model, effectively combining both precision and completeness in earth-  
 177 quake detection. These metrics underscore the robust performance of the EQT model in expanding the OVSICORI  
 178 earthquake catalog. By setting the appropriate probability threshold, it is possible to ensure high detection accuracy  
 179 and completeness, the 80% probability threshold was chosen as it balanced reducing false positives while maintaining  
 180 a high signal-to-noise ratio, important for analyzing low magnitude events.

### 181 **3. Methodology**

182 We expanded the work of van der Laet et al. (2021) by evaluating the uncertainties and consistency in earth-  
 183 quake detection carried out by EQT during two consecutive executions with the same parametrization and dataset.  
 184 We performed this task for each detection method in EQT: the complex method (Predictor) and the simplified method

(MseedPredictor). We used the seismic records from 5 stations operated by OVSICORI in the region surrounding the Poás Volcano in central Costa Rica. Since we wanted to reproduce the performance of both detection methods at each recording site, we generated a total of 4 executions per seismic station: 2 for the complex method and 2 for the simplified method.

For each station, we selected 24-hours of data following the occurrence of the Magnitude 5.5 mainshock and part of the aftershock sequence that occurred on February 18, 2023, along the Northeastern flank of the Poás Volcano, near the town of Cinchona, Alajuela. This sequence is shown as green circles in Figure 2, where the size of the circles represents earthquake magnitude and triangles correspond with the spatial distribution of broadband seismic stations around the study area. This earthquake sequence is aligned parallel to the January 2009, M6.2 Cinchona earthquake sequence (shown as light blue circles), one of the most devastating events in the history of Costa Rica. During this event, multiple earthquake-triggered landslides caused the loss of 25 lives, left 17 people missing, and resulted in significant damage to public and private infrastructure [Instituto Costarricense de Electricidad and Universidad de Costa Rica (2009)], including hydroelectric dams of the Costa Rican Institute of Electricity (ICE), such as the Toro II and Cariblanco, which were partially affected. Therefore, characterizing the 2023 sequence is necessary for a better understanding of the seismotectonics and earthquake potential in the region.

### 3.1. Computer architectures and EQT detection functions

For analyzing the data, we initially considered four different computational architectures to explore the performance of our methods. These included three GPUs and one CPU, all detailed in Table 2. After evaluating the GPU performance specifications listed in the table, we decided to concentrate exclusively on the NVIDIA V100 GPU. This choice was driven by the V100's superior performance across several key metrics, including processing speed, memory capacity, memory bandwidth, and overall efficiency, making it the most suitable option for our analyses. By selecting the best-performing architecture, we aim to ensure that our results are both robust and consistent, minimizing any variability that could arise from using less capable hardware.

Having selected the optimal hardware, we then focused on two primary earthquake detection functions:

The simplified execution method processes MiniSeed files from each station and runs a single pass without providing uncertainty estimates for the P and S phases or earthquake detection probabilities. This approach is suitable for larger datasets as it is more memory-efficient, bypassing the pre-processing step and working directly with the downloaded MiniSeed files.

In contrast, the complex execution method offers more detailed and customizable options. Although more demanding to implement, it allows for performance testing and the exploration of various parameter settings. This method requires pre-processed data and is better suited for smaller datasets, typically covering a period of a few days to a

<i>Architecture</i>	<i>Core clock speed</i>	<i>Main memory size</i>	<i>Memory clock speed</i>	<i>Memory bandwidth</i>	<i>Power consumption (TDP)</i>
<b>NVIDIA TESLA V100 PCIe</b>	1246 MHz	32 GB	1758 MHz	900.1 GB/s	250 Watt
<b>NVIDIA TESLA K40 PCIe</b>	745 MHz	12 GB	3004 MHz	288.4 GB/s	245 Watt
<b>NVIDIA TESLA P6</b>	1012 MHz	16 GB	6008 MHz	192.2 GB/s	90 Watt
<b>CPU Intel Xeon Silver 4214R</b>	2.40 GHz (24 cores)	128 GB	2933 MHz	107.3 GB/s	100 Watt

**Table 2**  
Specifications of the evaluated computational architectures.

<b>Parameter</b>	<b>Predictor</b>	<b>MseedPredictor</b>
Loss types	[binary_crossentropy, binary_crossentropy, binary_crossentropy]	[binary_crossentropy, binary_crossentropy, binary_crossentropy]
Loss weights	[0.02, 0.4, 0.58]	[0.02, 0.4, 0.58]
Batch size	500	500
Normalization mode	std	std
Estimate uncertainty	True	N/A
Number of Monte Carlo sampling	50	N/A
Overlap	0.9	0.9
Detection threshold	0.85	0.85
P threshold	0.9	0.9
S threshold	0.7	0.7
Use multiprocessing	True	N/A
gpuid	0	0
gpu limit	None	None
KeepPS	False	N/A
Allow only S	True	N/A
spLimit	60 seconds	N/A

**Table 3**  
Configuration parameters for Predictor and MseedPredictor execution methods.

216 month. Furthermore, the Predictor function supports lower threshold values for detection and picking, leveraging  
217 EQTransformer’s strong resistance to false positives.

218 Considering the existence of these two distinct methods, it becomes imperative to ensure uniform configuration for  
219 each execution. In Table 3 we provide a summary of the configuration parameters used for both methods.

220 The complex method incorporates Monte Carlo Dropout for both detection and probability estimation, using 50  
221 iterations. This number was determined by evaluating the percentage of matching events between experiments and  
222 observing its convergence. This approach is analogous to the Elbow method in clustering analysis, where the optimal  
223 number of clusters is identified by finding the point where the reduction in the sum of squared errors (SSE) slows  
224 significantly Humaira and Rasyidah (2020). Similarly, in our case, we identified the point where increasing the number  
225 of iterations leads to diminishing improvements in the percentage of matching events. Figure 3 shows this relationship,  
226 illustrating that with 50 iterations, we achieved over 90% matching accuracy. Beyond this point, additional iterations  
227 yielded progressively smaller gains, mirroring the behavior observed in the Elbow method when the SSE reduction

228 begins to taper off.

229 For each station, we analyzed the number of events detected as a function of time for the two equal and consecutive  
230 experiments. This allowed us to track down possible errors or variations in earthquake detection per site. Furthermore,  
231 we compared the number of events per hour for each station across the two experiments. This comparison helped to  
232 identify any specific hours during which differences occur, providing insights into the possible sources of discrepancy.

233 Finally, for each detection method, we compared the detection results from each experiment at each recording  
234 site, by applying a match filter algorithm to the detected origin time of the events, allowing a lag time of about  $\pm 10$   
235 seconds and ensuring that all detections were performed on the same station channel (East, North or Vertical). This  
236 comprehensive analysis allows us to understand the functionality and better interpret the results from EQT.

## 237 4. Results and discussion

238 As previously introduced, we selected the Northeastern flank of the Poás Volcano, near the town of Cinchona,  
239 Alajuela, Costa Rica, to evaluate the performance of the OKSP pipeline during the detection stage, as shown in Figure  
240 2.

241 We analyzed 24-hr time series from five broadband stations in the study area, using the two execution methods  
242 available within EQT and described in Table 3. Figure 4 presents the results for the seismic station VPTE, located  
243 at Poás Volcano, the closest station to the mainshock in this region. This figure illustrates the cumulative number of  
244 events detected as a function of time from 00:00 on February 18 to 00:00 on February 19, 2023. Figure 4a displays the  
245 outcomes using the complex method with Monte Carlo Dropout, while Figure 4b shows the results using the Simplified  
246 execution method.

247 We analyzed the data from all five stations similarly as shown in Figure 4, executing the detection process twice to  
248 facilitate a comparative study. Even though the input dataset, computer architecture, and the function parametrization  
249 were invariant, the Complex method yields fewer event detections with respect to the Simplified method.

250 The comparison between each run or experiment, shown as pink and purple lines in Figure 4, show clear evi-  
251 dence of non-determinism, regardless of the method used for earthquake detection. We noticed that for the Complex  
252 method, which relays on the Monte Carlo Dropout for discriminating detections, the overall count of events presents  
253 less variance with respect to the Simplified method.

254 For instance, for the same station, VPTE, the relative difference in earthquake count for the Complex method  
255 resulted in  $\pm 3$  events, while for the Simplified method, the detection difference resulted in 1 order of magnitude higher  
256 ( $\pm 30$  events). Our results show that for both detection methods, the second experiment, or execution, resulted in a  
257 higher number of events detected compared to the first experiment. However, this pattern doesn't remain consistent as  
258 we run more experiments. In fact, for the other analyzed stations, sometimes Experiment 1 had more detections than

**Table 4**

Events detected at multiple time-intervals

Execution method		06:00	12:00	18:00	23:59
Simplified	Exp1	156	395	565	661
	Exp2	167	427	586	691
Complex	Exp1	11	46	73	81
	Exp2	13	47	75	83

259 Experiment 2 for both methods, so we don't observe a clear behavior, with some randomness occurring.

260 As displayed in Figure 4, the difference in the number of detections are scattered throughout the 24-hour analysis  
 261 period, inducing a time shift between the pink and purple curves for both detection methods. However, for the simplified  
 262 method, a significant divergence begins around 6:00 am, where the differences between the two experiments increase  
 263 noticeably.

264 We include zoomed-in plots in Figure 4 in order to reinforce the observed variability obtained with both algorithms.  
 265 For the Complex method, for instance, the difference remains relatively constant within the zoomed-in time range,  
 266 whereas for the simplified method, the difference increases within this area. Also, during the zoomed-in period, a  
 267 specific pattern in the number of events was observed, with the main event occurring at 08:24 UTC. For both methods,  
 268 the number of events converged around this time. However, for the Complex method, the number of events remained  
 269 relatively constant between experiments, while the Simplified method showed significant divergence for the rest of  
 270 the day. The maximum difference in events also appeared for the Simplified method, indicating the need for further  
 271 analysis.

272 To represent these changes, we considered specific time points: 6:00, 12:00, 18:00, and 23:59, as summarized in  
 273 Table 4 for the VPTE station.

274 Table 4 reveals that the number of events decreases by approximately tenfold when using the Complex method,  
 275 despite consistent detection parameters and conditions. It is important to recall Table 3, where the threshold was kept  
 276 constant for comparison purposes. However, lowering the threshold for the Complex method could result in a higher  
 277 number of detected events.

278 Additionally, our observations highlight a general decrease in the number of detections when comparing the two  
 279 methods, despite using the same model and parameters. The crucial difference is that the Complex method utilizes  
 280 iterations of Monte Carlo dropout during the prediction stage. The changes observed in the Simplified method, espe-  
 281 cially in the zoomed-in areas, suggest a significant impact on detection outcomes.

282  
 283 Figures 5 and 6 show a similar comparison between the number of seismic events detected per hour using both  
 284 earthquake detection methods (3) across the five seismic stations described above and shown in Figure 2. The com-



285 parison is presented through subplots (A, B, C, D, E) for each station, and a general heatmap (F) that illustrates the  
286 difference in the number of events detected between two consecutive experiments using both execution methods. In  
287 the heat map, the color indicates the count difference in event detections between the 2 executions. This value is also  
288 indicated within each cell.

289 The differences in the number of detected events across the two experiments, indicate that, either of the detection  
290 methods introduces a certain level of variability, with the Complex method being more reproducible or less variable  
291 than the Simplified method by  $\sim 1$  order of magnitude.

292 This non-determinism may result from the inherent stochastic nature of the detection methods or any potential issues  
293 in the computational process. For the case of the Complex method, the random sampling process inherent to Monte  
294 Carlo Dropout results in different subsets of neurons being dropped out. This means that, even with identical input  
295 data and model parameters, the method may produce slightly different outputs in different runs, leading to variability  
296 in the number of detected seismic events. Since dropout is applied randomly in each forward pass, the predictions (and  
297 thus the detected events) can vary between runs. This stochastic nature is intended to simulate the model's behavior  
298 and also quantify uncertainties in event detections within the AI framework.

299 We developed a match filter technique to evaluate the consistency in event detection for all seismic stations with  
300 the aim of exploring time-dependent appearance of new detections, false positives and plausible temporal variations  
301 in the number of events detected. For this, we determine whether two events are identical across different executions  
302 by comparing the event start time ( $\pm 10s$ ), station, and detection channel (E, N or Z). We tested the match filter method  
303 for the two consecutive experiments either for the Complex and the Simplified method and computed the matching  
304 percentage between the experiments. Our findings are summarized in Figure 7.

305 According to the filtering criteria described in the methods section, the Complex detection method shows that 85%  
306 to 95% of the events are identical in two different executions. In contrast, the Simplified method exhibits significantly  
307 lower performance, with matched events ranging from 60% to 70%.

308 This significant difference in the matching percentage provides critical insights. For instance, for quick and straight-  
309 forward detections, the Simplified execution method is effective, offering a reasonable matching rate between exper-  
310 iments. However, it also raises a concern, giving that about 30% to 40 % of the detections may be false positives  
311 and thus, results must be interpreted with caution. On the other hand, the Complex execution method substantially  
312 increases the matching percentage, indicating a more conservative approach. Although it detects fewer events, the  
313 majority of these events are reproducible across different executions, which is crucial for establishing the reliability of  
314 the tool when used by seismological research centers.

## 5. Conclusions

The results obtained in this study reveal significant differences in seismic event detection when comparing the Simplified execution method and Complex execution method. The Complex method consistently detects fewer events, approximately one-tenth compared to simplified. This outcome underscores the impact of the iterative Monte Carlo dropout used in the Predictor method, which appears to enhance model robustness by reducing false positives.

Moreover, there is a notable difference in the consistency of event detection between the two methods. The Complex method exhibits minimal variability between repeated runs, with differences typically near zero and a maximum of two events detected in our tests. In contrast, the Simplified method shows considerable variability, with differences reaching up to one order of magnitude in some cases. This suggests that the Complex method provides more reliable and reproducible results, which are crucial for accurate seismic analysis.

Regarding temporal patterns and major events, both methods tend to converge on the number of events detected up to the mainshock. However, after this event, the Simplified execution method shows a significant divergence in the number of events detected throughout the remainder of the day, while the Complex execution method maintains this divergence on a much smaller scale. This indicates that although both methods are effective in identifying major events, the Complex execution method sustains more consistent performance over extended periods.

Donut plots comparing the percentage of matched events between the two methods reveal that the Complex method achieves a higher match rate (85% to 95%) compared to the Simplified method (60% to 70%). This suggests that while the Predictor method detects fewer events, it does so with greater reliability and consistency in identifying the same events across repeated runs.

Our findings are critical for optimizing the use of EQTransformer and AI tools in seismological research. The Complex execution method, with its enhanced consistency and reliability, is better suited for applications requiring high precision and reproducibility, making it more recommended for professional use, such as in seismological research institutions. Meanwhile, the Simplified execution method, despite its higher event detection rate, may be more prone to variability and false positives. However, it offers the advantage of being easier to use and computationally lighter, making it suitable for non-professional tasks, such as training, academic purposes, and other less demanding applications.

## 6. Future Work

In this study, we have demonstrated the presence of a certain level of non-determinism in earthquake detection, which, while mitigated by the use of Monte Carlo Dropout in the Complex method, still results in a degree of irreproducibility, as observed in several Figures. Although the Complex method improves the reliability of detections, it does not entirely eliminate variability in the results.

346 A crucial direction for future work involves identifying the sources of randomness within the EQTransformer tool.  
347 Understanding these sources will be key to further reducing the level of uncertainty and enhancing the reproducibility  
348 of the detection process. By addressing this issue, we can refine the model's performance, leading to more consistent  
349 and dependable earthquake detection outcomes across different datasets and operational conditions.

## 350 **7. Acknowledgments**

351 This research was partially supported by a machine allocation on Kabré supercomputer at the Costa Rica National  
352 High Technology Center.

## 353 **Code Availability**

354 This research utilized multiple codes and tools, some of which were developed by us, in addition to the use of  
355 EQTransformer Mousavi et al. (2020). As this research is an extension of the OKSP workflow developed in 2021  
356 van der Laet et al. (2021), we provide the necessary tools, code, and data to reproduce our results.

## 357 **Hardware Requirements**

- 358 • **Operating System:** Linux 64-bit (cluster, server, or personal computer).
- 359 • **GPU Recommendation:** We recommend using an NVIDIA GPU to achieve faster results.

## 360 **Programming Language**

- 361 • **Python:** All scripts and tools are developed in Python 3.

## 362 **Software Requirements**

- 363 • **Conda Environment:** We recommend working within a Conda environment for consistency and ease of repro-  
364 duction. To facilitate this, we provide a clone of our environment. Detailed instructions for setting up Conda  
365 can be found in the following tutorial: [https://github.com/um-dang/conda\\_on\\_the\\_cluster.git](https://github.com/um-dang/conda_on_the_cluster.git)
- 366 • **EQTransformer:** The EQTransformer tool can be accessed by cloning the following repository: [https://](https://github.com/smousavi05/EQTransformer.git)  
367 [github.com/smousavi05/EQTransformer.git](https://github.com/smousavi05/EQTransformer.git)  
368 **Note:** We strongly recommend using our provided Conda environment as it contains updated software libraries  
369 that we have actively used in this research.
- 370 • **Research Source Code:** The source code necessary for the detection stage, based on the OKSP pipeline van der  
371 Laet et al. (2021), along with additional code and data required for reproducing the results, is available.  
372 **Note:** A README file is included in the repository, providing step-by-step instructions for use.  
373 The source code is available for download at the following link: [https://github.com/SebasGamboa10/](https://github.com/SebasGamboa10/Reproducibility-and-Uncertainty-Assessment-in-EQTransformer.git)  
374 [Reproducibility-and-Uncertainty-Assessment-in-EQTransformer.git](https://github.com/SebasGamboa10/Reproducibility-and-Uncertainty-Assessment-in-EQTransformer.git)

## 375 **Contact Information**

376 For any inquiries or additional support, please contact us at:

- 377 • **Email:** [sgamboa@cenat.ac.cr](mailto:sgamboa@cenat.ac.cr)
- 378 • **GitHub:** <https://github.com/SebasGamboa10>
- 379 • **Phone:** +506 6098 1011

## References

- Arrowsmith, S.J., Trugman, D.T., MacCarthy, J., Bergen, K.J., Lumley, D., Magnani, M.B., 2022. Big data seismology. *Reviews of Geophysics* 60, e2021RG000769.
- Castillo, E., Siervo, D., Prieto, G.A., 2024. Colombian Seismic Monitoring Using Advanced Machine-Learning Algorithms. *Seismological Research Letters* URL: <https://doi.org/10.1785/0220240036>, doi:10.1785/0220240036.
- Gal, Y., Ghahramani, Z., 2016. Dropout as a bayesian approximation: Representing model uncertainty in deep learning. URL: <https://arxiv.org/abs/1506.02142>, arXiv:1506.02142.
- Gürsoy, G., Varol, A., Nasab, A., 2023. Importance of machine learning and deep learning algorithms in earthquake prediction: A review, in: 2023 11th International Symposium on Digital Forensics and Security (ISDFS), pp. 1–6. doi:10.1109/ISDFS58141.2023.10131766.
- Hassan, R., Hejrani, B., Zhang, F., Gorbatov, A., Medlin, A., 2020. High-performance seismological tools (HiPerSeis). *Geoscience Australia* Canberra.
- Humaira, H., Rasyidah, R., 2020. Determining the appropriate cluster number using elbow method for k-means algorithm, *EAI*. doi:10.4108/eai.24-1-2018.2292388.
- Instituto Costarricense de Electricidad, Universidad de Costa Rica, 2009. El terremoto de cinchona del 8 de enero de 2009 - informe completo. *Red Sismológica Nacional (RSN: UCR-ICE)*, 1–132.
- Jiang, C., Fang, L., Fan, L., Li, B., 2021. Comparison of the earthquake detection abilities of phasenet and eqtransformer with the yangbi and maduo earthquakes. *Earthquake Science* 34, 425–435. URL: <https://www.sciencedirect.com/science/article/pii/S1674451922000581>, doi:<https://doi.org/10.29382/eqs-2021-0038>.
- van der Laet, L., Baldares, R.J.L., Chaves, E.J., Meneses, E., 2021. Oksp: A novel deep learning automatic event detection pipeline for seismic monitoring in costa rica. URL: <https://arxiv.org/abs/2109.02723>, arXiv:2109.02723.
- Montero, W., Denyer, P., Barquero, R., Alvarado, G., Cowan, H., 1998. Map of Quaternary faults and folds of Costa Rica. Technical Report.
- Mousavi, S.M., Ellsworth, W.L., Zhu, W., Chuang, L.Y., Beroza, G.C., 2020. Earthquake transformer—an attentive deep-learning model for simultaneous earthquake detection and phase picking. *Nature Communications* 11, 1–12.
- Pita-Sllim, O., Chamberlain, C.J., Townend, J., Warren-Smith, E., 2023. Parametric Testing of EQTransformer’s Performance against a High-Quality, Manually Picked Catalog for Reliable and Accurate Seismic Phase Picking. *The Seismic Record* 3, 332–341. URL: <https://doi.org/10.1785/0320230024>, doi:10.1785/0320230024.
- Protti, M., Gündel, F., McNally, K., 1994. The geometry of the wadati-benioff zone under southern central america and its tectonic significance: results from a high-resolution local seismographic network. *Physics of the Earth and Planetary Interiors* 84, 271–287. URL: <https://www.sciencedirect.com/science/article/pii/0031920194900469>, doi:[https://doi.org/10.1016/0031-9201\(94\)90046-9](https://doi.org/10.1016/0031-9201(94)90046-9).
- Spassiani, I., Sebastiani, G., 2016. Exploring the relationship between the magnitudes of seismic events. *Journal of Geophysical Research: Solid Earth* 121, 903–916.
- Styron, R., García-Pelaez, J., Pagani, M., 2020. Ccaf-db: the caribbean and central american active fault database. *Natural Hazards and Earth System Sciences* 20, 831–857.

413 **List of Figures**

414 1 OKSP pipeline. A schematic representation of the earthquake detection and phase identification pro-  
 415 cess at the Costa Rica High Technology Center (CeNAT). This system utilizes three-component seis-  
 416 mic data from OVSICORI-UNA to automatically generate a seismic catalog. . . . . 15

417 2 Map of the study area. The map is showing the spatial distribution of the earthquake sequence gener-  
 418 ated by the February 18, 2023, M5.5 mainshock and its aftershocks (green circles) and its proximity  
 419 to the January 8, 2009, M6.2 Cinchona earthquake sequence (light blue). In this figure, the size of the  
 420 circles represent the magnitude of the earthquakes, while triangles correspond with the stations used  
 421 for analyzing the seismic data in this study . . . . . 16

422 3 Figure showing the matching percentage average between to experiments vs Iterations using Monte  
 423 Carlo Dropout. Note that with 50 iterations, we achieved a matching percentage higher than 90%.  
 424 This indicates that, beyond this point, further iterations yield progressively smaller improvements in  
 425 matching accuracy. . . . . 17

426 4 Results from consecutive experiments performed using seismic station VPTE. For these experiments  
 427 the parametrization and data were invariant. In panel a), we show the cumulative number of events  
 428 detected as function of time using the Predictor method of EQT, where purple and pink lines indicate  
 429 the first and second run, respectively. Similarly, panel b) highlight the results obtained for the same  
 430 station, VPTE, but using the MseedPredictor function. The Purple and pink lines indicate the first and  
 431 second experiment. Note the difference in the number of detections for both methods. . . . . 18

432 5 A, B, C, D, E, Comparison plots of the number of events per hour for two exactly equal experiments  
 433 using five stations. F, a heatmap of the difference of events per hour between the two experiments,  
 434 **using complex execution method.** . . . . . 19

435 6 A, B, C, D, E, Comparison plots of the number of events per hour for two exactly equal experiments  
 436 using five stations. F, a heatmap of the difference of events per hour between the two experiments,  
 437 **using simplified execution method.** . . . . . 20

438 7 Donut Plot representing the matching percentage between experiments for each station. a) Using com-  
 439 plex method. b) Using simplified method. . . . . 21

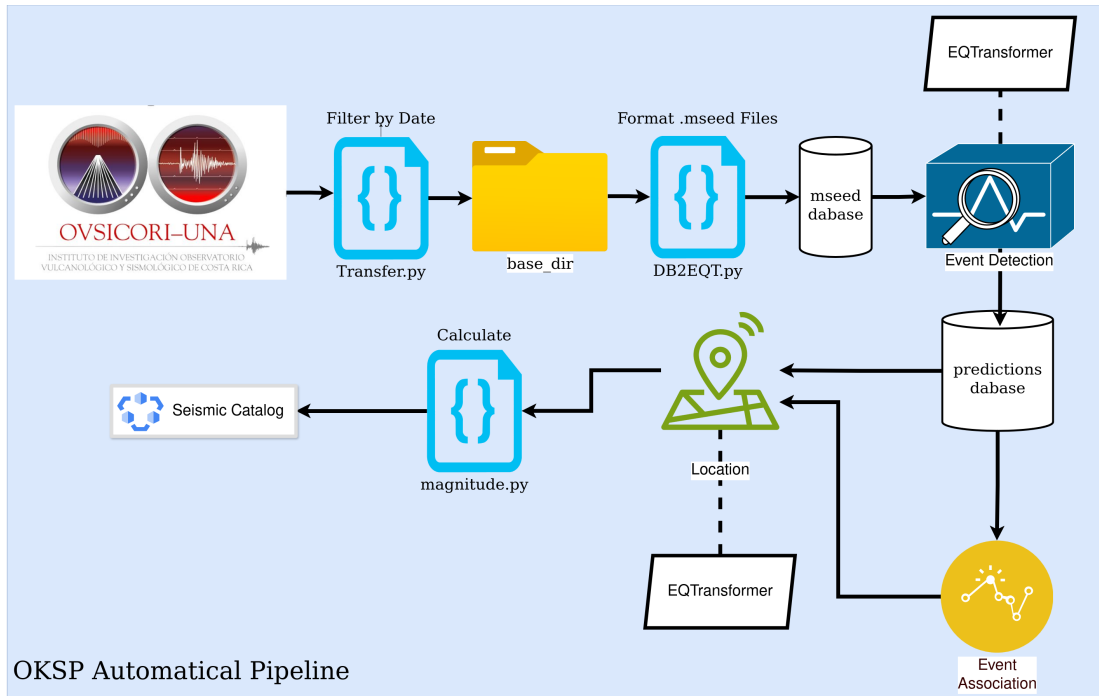


**Figure 1:** OKSP pipeline. A schematic representation of the earthquake detection and phase identification process at the Costa Rica High Technology Center (CeNAT). This system utilizes three-component seismic data from OVSICORI-UNA to automatically generate a seismic catalog.

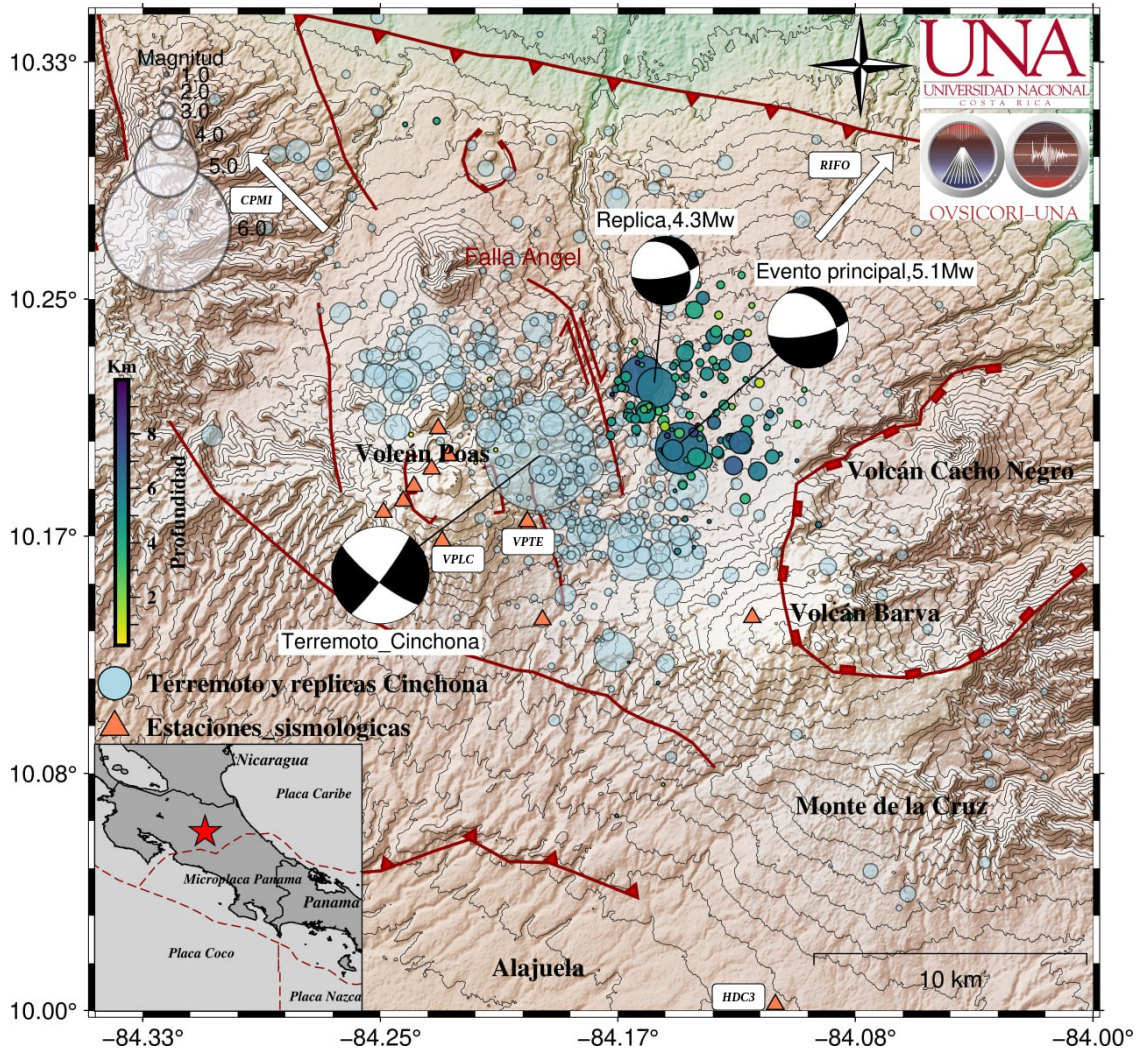


**Figure 2:** Map of the study area. The map is showing the spatial distribution of the earthquake sequence generated by the February 18, 2023, M5.5 mainshock and its aftershocks (green circles) and its proximity to the January 8, 2009, M6.2 Cinchona earthquake (light blue). In this figure, the size of the circles represent the magnitude of the earthquakes, while triangles correspond with the stations used for analyzing the seismic data in this study



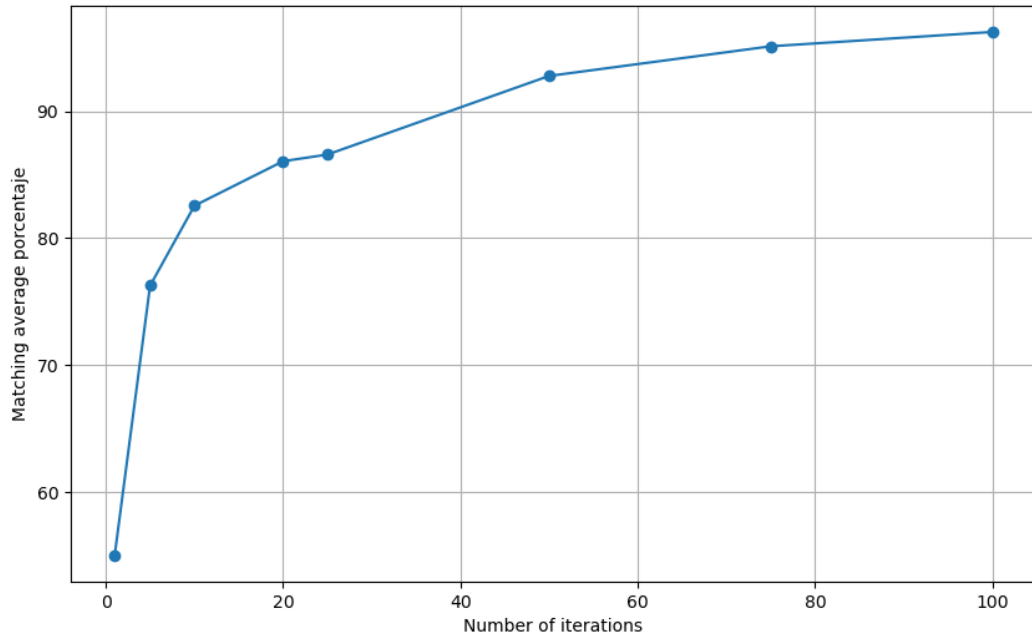


**Figure 3:** Figure showing the matching percentage average between to experiments vs Iterations using Monte Carlo Dropout. Note that with 50 iterations, we achieved a matching percentage higher than 90%. This indicates that, beyond this point, further iterations yield progressively smaller improvements in matching accuracy.

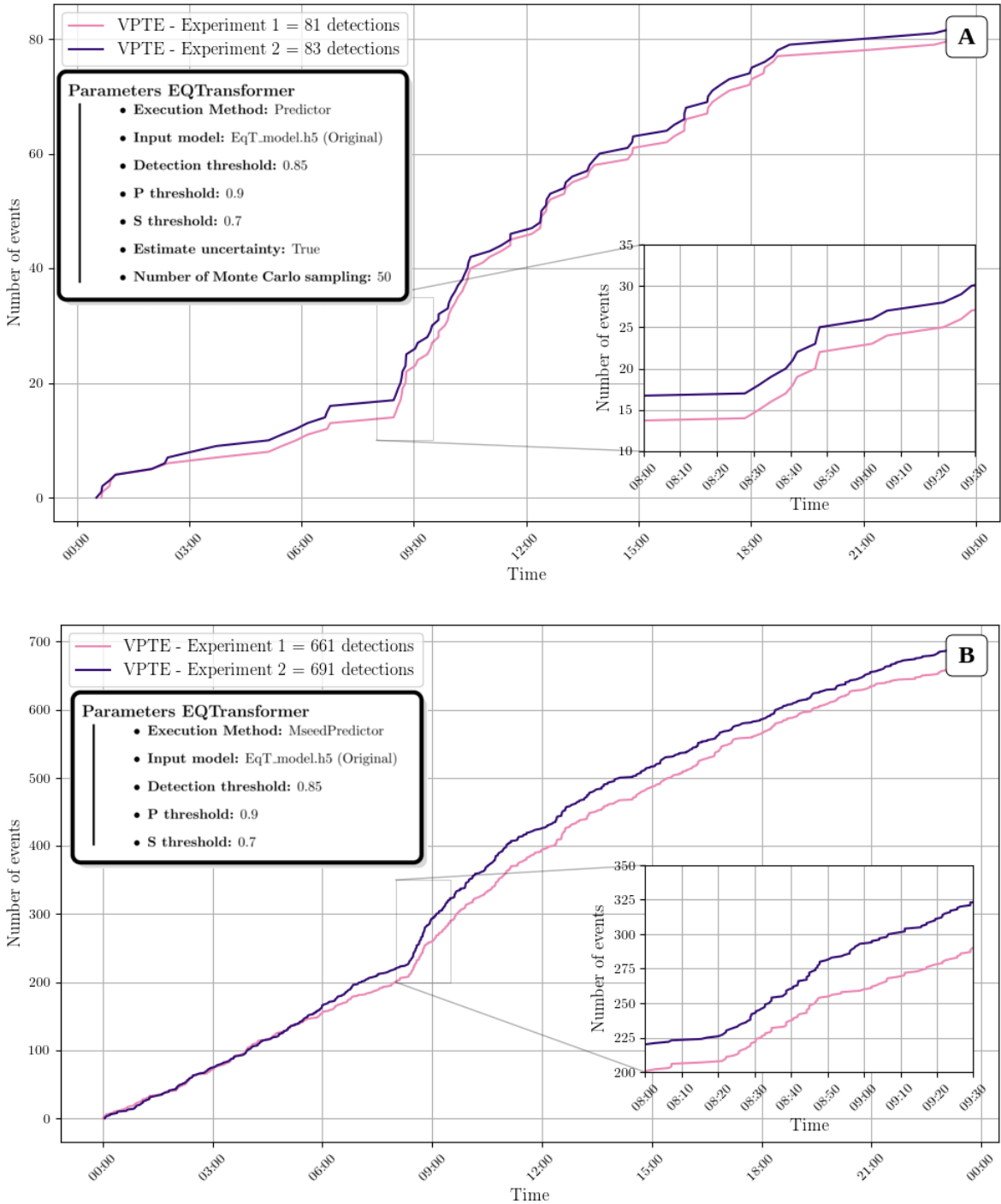


**Figure 4:** Results from consecutive experiments performed using seismic station VPTE. For these experiments the parametrization and data were invariant. In panel a), we show the cumulative number of events detected as function of time using the Predictor method of EQT, where purple and pink lines indicate the first and second run, respectively. Similarly, panel b) highlight the results obtained for the same station, VPTE, but using the MseedPredictor function. The Purple and pink lines indicate the first and second experiment. Note the difference in the number of detections for both methods.

## Exploring reproducibility in IA earthquake detection

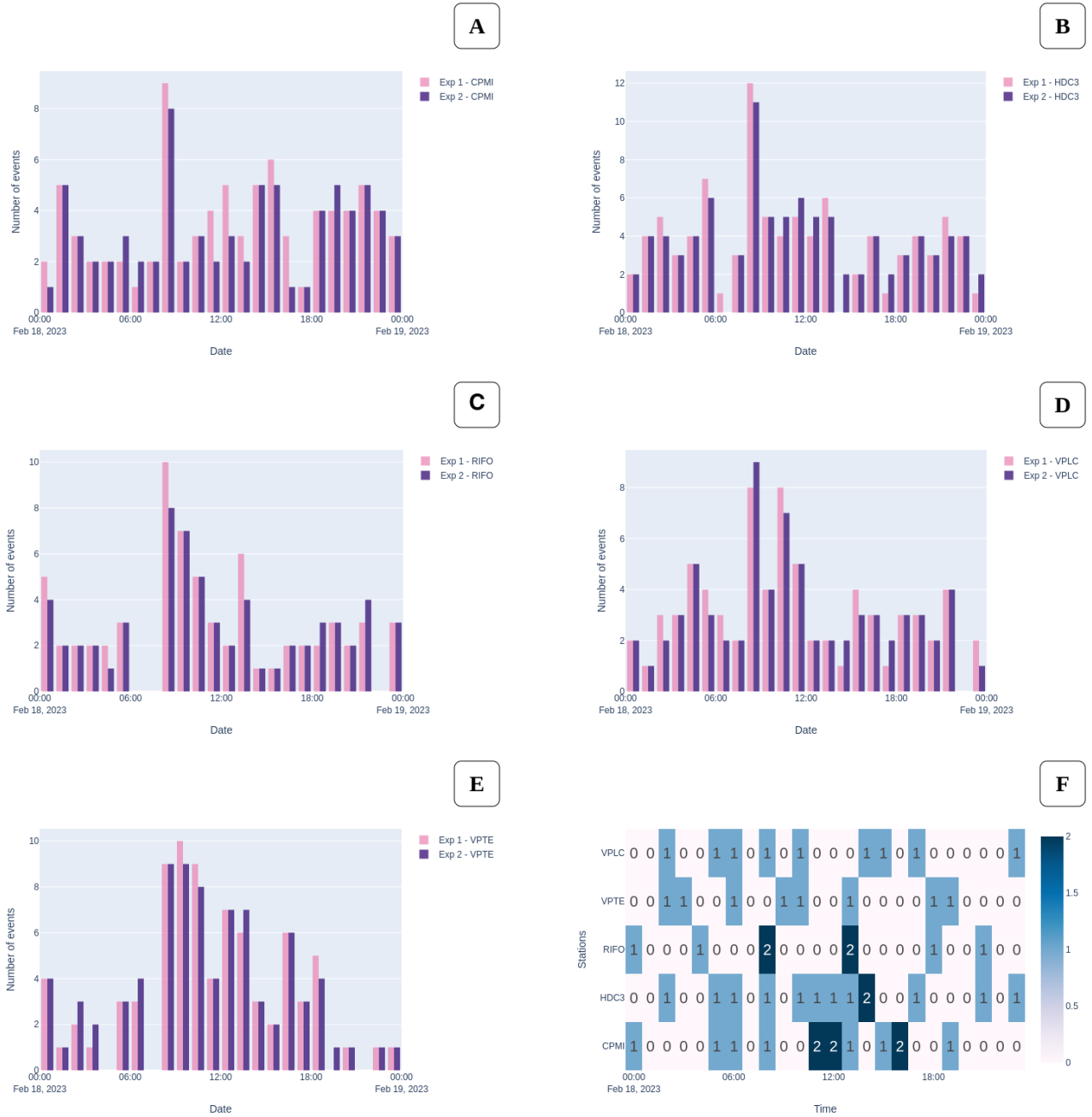


**Figure 5:** A, B, C, D, E, Comparison plots of the number of events per hour for two exactly equal experiments using five stations. F, a heatmap of the difference of events per hour between the two experiments, **using complex execution method**.

## Exploring reproducibility in IA earthquake detection

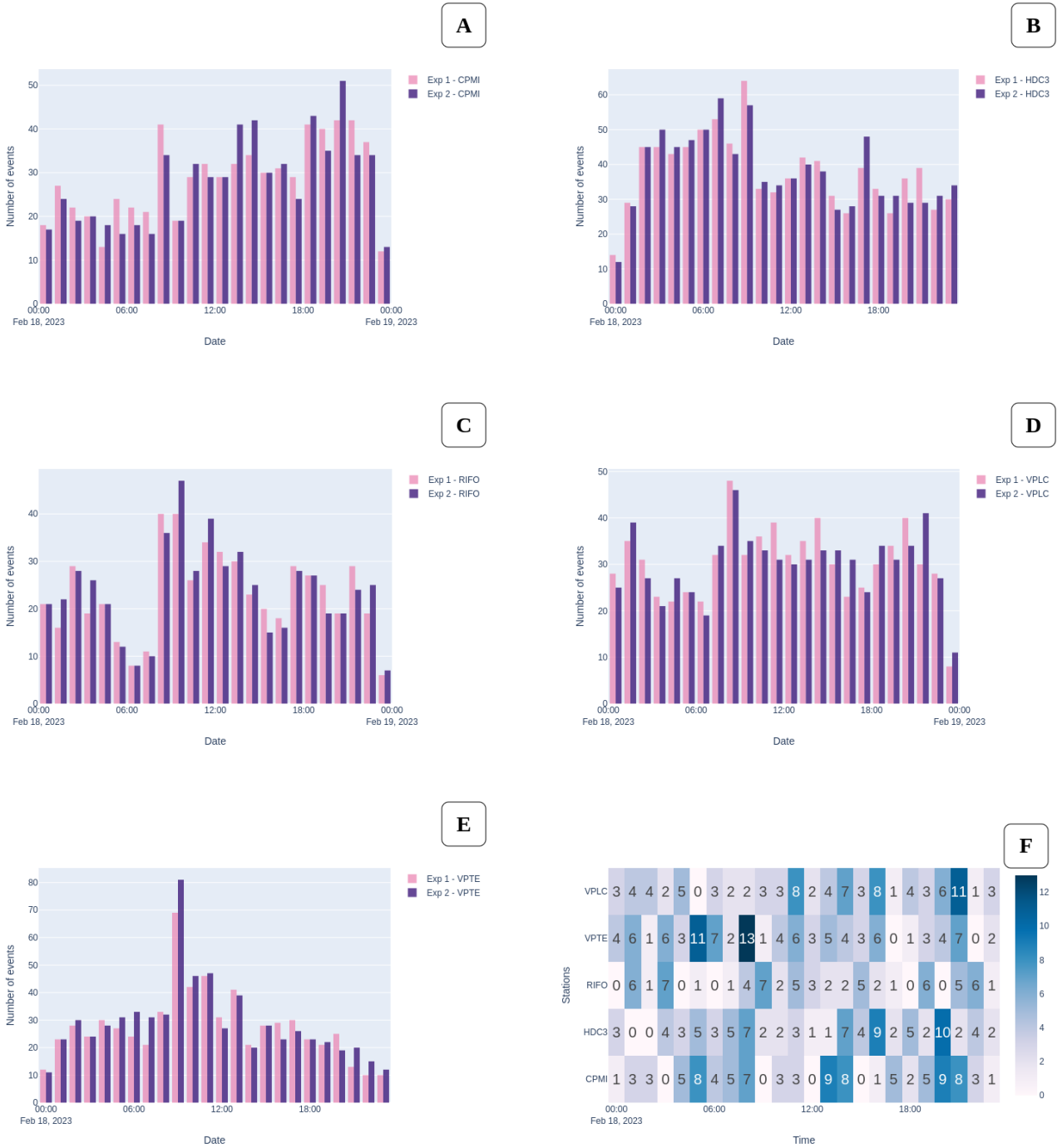


**Figure 6:** A, B, C, D, E, Comparison plots of the number of events per hour for two exactly equal experiments using five stations. F, a heatmap of the difference of events per hour between the two experiments, using simplified execution method.

## Exploring reproducibility in IA earthquake detection

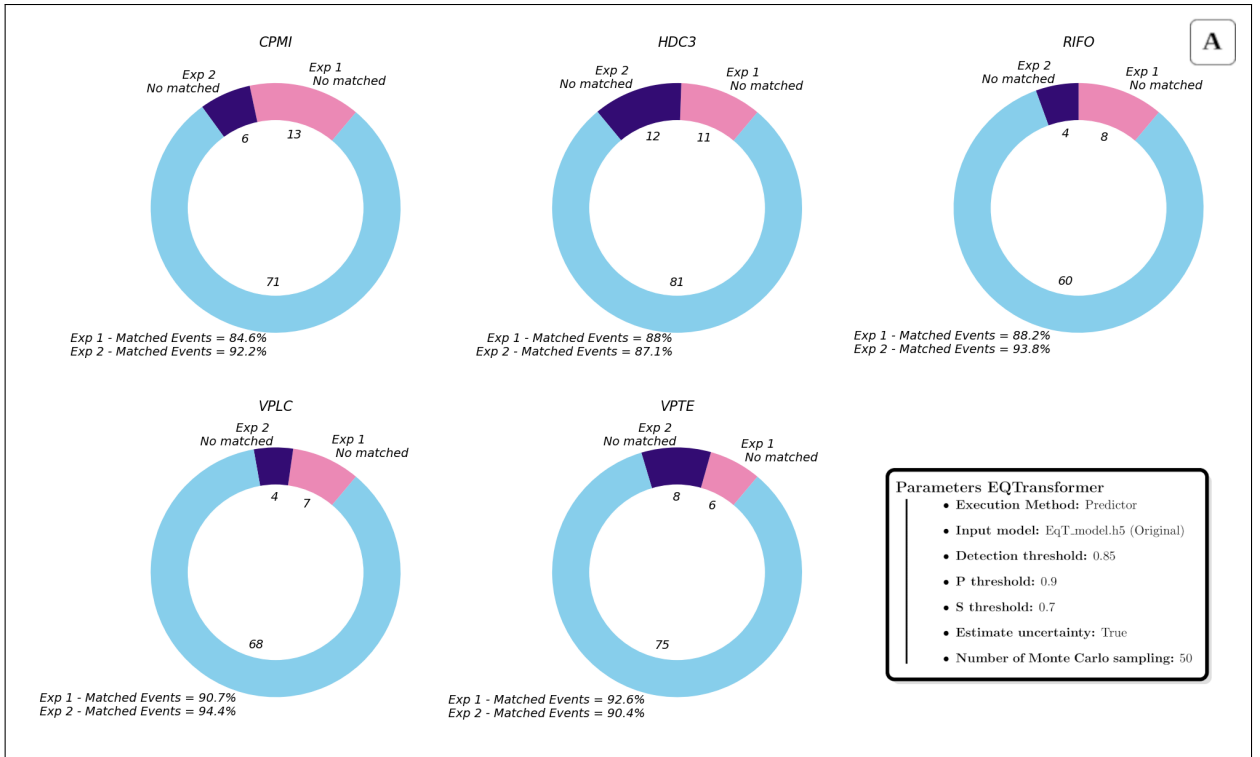


**Figure 7:** Donut Plot representing the matching percentage between experiments for each station. a) Using complex method. b) Using simplified method.